

# Comparative Study of Adaptive Beam-Steering and Adaptive Modulation-Assisted Dynamic Channel Allocation Algorithms

Jonathan Blogh, Peter. Cherriman, and Lajos Hanzo, *Senior Member, IEEE*

**Abstract**—A range of dynamic channel allocation (DCA) algorithms, namely, distributed control and locally distributed control assisted DCA arrangements, are studied comparatively. The so-called locally optimized least interference algorithm (LOLIA) emerges as one of the best candidates for future mobile systems, supporting more than twice the number of subscribers in comparison to conventional fixed channel allocation (FCA). It can also cope with unexpected large increases in teletraffic demands while requiring no tedious frequency planning. This is achieved at the cost of more complex call setup and control, and the requirement of fast backbone networks for base station–base station signalling. Adaptive antennas are shown to significantly enhance the capacity of both the LOLIA and FCA-based networks, especially when used in conjunction with adaptive modulation techniques.

**Index Terms**—Adaptive arrays, adaptive modulation, beam steering, dynamic channel allocation (DCA), smart antennas, wireless networking.

## I. BACKGROUND

THE recently emerging micro/picocellular frequency reuse structures increase the user capacity and area spectral efficiency of the system, although often at the cost of reduced frequency reuse distance and hence increased cochannel interference. Sectorization techniques [1], interference cancellation [2], or adaptive antennas [3]–[5] have been proposed for mitigating the cochannel interference. In small-cell environments, the handover process is critical, as highlighted by Tekinay *et al.* [6], [7], while the associated issues of timeslot reassignment were studied by Bernhardt [8].

This paper is concerned with the comparative study of dynamic channel allocation (DCA) algorithms [9]–[12], many of which were proposed and studied in terms of the achievable grade-of-service (GOS) by Chuang *et al.* throughout the past few years. In this paper, in addition to the GOS, we attempt to provide a performance comparison in terms of the carried teletraffic, call blocking probability, call dropping probability, probability of low-quality access, and outage probability for a range of DCA techniques under identical conditions, where all users seamlessly roam across the simulation area rather than simply assigning them to arbitrary, uncorrelated, but essentially

stationary random positions. It is also demonstrated that the proposed burst-by-burst adaptive modulation scheme [13] results in substantial teletraffic performance improvements.

This paper is structured as follows. Section II describes the DCA algorithms involved in the comparisons, while Section III–A introduces the simulation conditions, such as performance metrics, the nonuniform traffic model, and system parameters employed. The performance comparisons of Section IV constitute the bulk of this paper, leading to the conclusions in Section V.

## II. DYNAMIC CHANNEL ALLOCATION ALGORITHMS

We investigated both distributed and locally distributed DCA algorithms, which are described in Sections II-A and II-B, respectively. In this section, we mainly follow the approach of Chuang [9]–[11], who has pioneered the performance characterization of DCA techniques throughout the past few years.

### A. Distributed DCA Algorithms

In this section, we highlight the four distributed DCA algorithms that we have studied comparatively. The least interference algorithm (LIA)—which was also studied by Chuang in terms of the grade of service [11]—always assigns the channel suffering from the least interference, which minimizes the system's interference load at low traffic loads. However, at high traffic loads, the LIA algorithm will still attempt to allocate a channel to a new call, even when all the slots have a high level of interference, which increases the total interference of the system. A refined version of the LIA algorithm, namely, the least interference below threshold algorithm (LTA) [11], attempts to reduce the interference caused by the LIA algorithm at high loads, by blocking calls from using those channels, where the interference is deemed excessive for the transceiver, in order to sustain adequate communications quality. Hence, the LTA algorithm attempts to minimize the overall interference in the system while maintaining the targeted call quality.

The highest (or most) interference below threshold algorithm (HTA or MTA) [11] allocates the most interfered channel, whose interference is below the maximum tolerable interference threshold, which is determined by the transceiver's interference resilience. Hence, instead of minimizing the interference, this technique maximizes the spectral efficiency.

Lastly, the lowest frequency below threshold algorithm (LFA) [11], which was also studied by Chuang, is a relative of the

Manuscript received December 18, 1998; revised August 14, 2000. This work was supported by the European Commission in the framework of the TRUST Project.

The authors are with the Department of Electronics and Computer Science, University of Southampton, Southampton SO17 1BJ, U.K. (e-mail: <http://www-mobile.ecs.soton.ac.uk>; [pjc@ecs.soton.ac.uk](mailto:pjc@ecs.soton.ac.uk); [lh@ecs.soton.ac.uk](mailto:lh@ecs.soton.ac.uk)).

Publisher Item Identifier S 0018-9545(01)03222-4.

LTA algorithm, attempting to reduce the number of carrier frequencies used simultaneously, requiring on average a reduced number of transceivers at each basestation. The algorithm allocates the least interfered channel below the maximum tolerable interference threshold while also attempting to reduce the number of carrier frequencies used. Therefore, no new carrier frequency is assigned from the set of carriers, unless all of the available timeslots on the currently used carrier frequencies have too high a level of interference. In the next section, we describe the two locally distributed DCA algorithms, whose performance we have compared to the above algorithms using simulations.

### B. Locally Distributed DCA Algorithms

The locally optimized least interference algorithm (LOLIA) attempts to reduce the overall interference in a system, like the LIA and LTA, while the locally optimized most interference algorithm (LOMIA) improves the spectral efficiency similarly to the HTA. Specifically, the LOLIA and LOMIA exploit the channel assignment information provided by neighboring basestations in order to improve their DCA decisions.

More explicitly, the LOLIA always assigns the least interfered channel, unless it is used in the nearest  $n$  neighboring cells by another subscriber. However, the larger that  $n$  is, the higher the number of blocked calls, since there are fewer available channels that are not used in the nearest  $n$  base stations. Fig. 1 shows the arrangement of neighboring cells for  $n = 7$ .

The  $n$  parameter of the algorithm effectively imposes a minimum reuse distance constraint upon the algorithm. By contrast, the LOMIA picks the most interfered channel, provided that this channel is not used in the nearest  $n$  neighboring cells. The LOLIA and LOMIA are similar to those proposed by Del Re *et al.* [14] and by ChihLin *et al.* [15].

## III. SIMULATION CONDITIONS

### A. Performance Metrics

The following performance metrics have been widely used in the literature and were also advocated by Chuang [11]:

- 1) new call blocking probability  $P_B$ ;
- 2) call dropping or forced termination probability  $P_D$  or  $P_{FT}$ ;
- 3) probability of low-quality connection  $P_{low}$ , quantifying the chances that either the uplink or downlink signal quality is below the level required by the specific transceiver to maintain a given target performance;
- 4) probability of outage  $P_{out}$ , defined as the probability that the signal-to-interference-plus-noise ratio (SINR) value is below the value where the call is deemed to be in outage, as described in Section III-C;
- 5) GOS, defined by Cheng and Chuang [11] as

$$\begin{aligned} \text{GOS} &= P\{\text{unsuccessful or low-quality call accesses}\} \\ &= P\{\text{call is blocked}\} + P\{\text{call is admitted}\} \\ &\quad \times P\{\text{low signal quality and call is admitted}\} \\ &= P_B + (1 - P_B)P_{low}. \end{aligned} \quad (1)$$

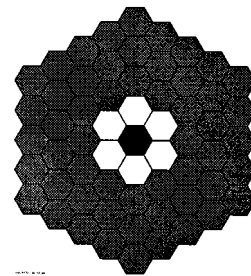


Fig. 1. Frequency-reuse “exclusion zone” employed by the LOLIA and LOMIA. This cell layout also demonstrates the nonuniform traffic conditions used in the forthcoming performance comparisons, exhibiting a traffic “hot spot” in the central cell (black) and a “warm spot” (white cells) surrounding it. Mobiles in the gray cells move at the standard speed of 13.4 m/s (30 mi/h). Mobiles in the white (“warm spot”) cells can move at a speed of 9 m/s (20 mi/h). Mobiles in the black “hot-spot” cell are limited to a speed of 4 m/s (9 mi/h).

### B. Beamforming

Since cellular networks are generally interference limited, the interference reduction capabilities of adaptive antenna arrays render them particularly suitable for this application [16], [17]. Adaptive antennas reduce the levels of cochannel interference by exploiting the spatial dimension, i.e., the physical separation between users, and thus may increase the network capacity, or the call quality. Assuming that each mobile station may be uniquely identifiable, a beamforming algorithm may be invoked in order to calculate the antenna array’s receiver weights, so as to maximize the received SINR. However, in a frequency-division duplexed (FDD) system, the up- and downlink channels are generally uncorrelated; hence the antenna array weights calculated for the uplink are not directly applicable to the downlink situation. A feedback loop from the mobile station to the base station has been proposed [18], [19], thus enabling the transmit antenna array weights to be adjusted. An alternative solution is to use time-division duplexing (TDD) with adjacent up- and downlink slots and a sufficiently short dwell time, such that the up- and downlink channels do not vary significantly, therefore allowing the complex conjugate of the receive antenna weights to be used as the transmit antenna weights [16].

The receiver antenna array weights were calculated employing the sample matrix inversion (SMI) algorithm [16], using a binary phase-shift keying (BPSK) modulated reference signal of eight bits, chosen as a compromise between complexity and the quality of the estimation of the received signal’s covariance matrix. It was assumed that the up- and downlink channels were identical, thus enabling the same antenna pattern to be used in both transmit and receive modes. This assumption should therefore give an upper limit to the performance gains that may be achieved using an adaptive antenna array. The array consisted of four antenna elements in a linear array configuration with  $\lambda/2$  element spacing.

### C. System Parameters

The performance of the various channel allocation algorithms was investigated in a GSM-like [20] microcellular system, the parameters of which are defined in Table I. The propagation environment was modeled using the power pathloss model with a pathloss exponent of  $-3.5$ . Jakes’ model [21] was used,

TABLE I  
GSM-LIKE DCA SYSTEM PARAMETERS

Parameter	Value	Parameter	Value
Noise floor	-104dBm	Pathloss Exponent	-3.5
Multiple Access	FDMA/TDMA	Number of timeslots	8
Frame length	0.004615s	Number of carriers	7
BS transmit power	10dBm	MS transmit power	10dBm
Average call-length	60s	Average inter-call-time	300s
MS speed (uniform traffic)	13.4m/s	MS speed (nonuniform traffic)	$\leq 13.4\text{m/s}$
Number of basestations	49	Max new-call queue-time	5s
Handover hysteresis	2dB	Cell radius	218m

when necessary, to generate the log-normal shadow fading, with random time offsets used for the different subscribers. The mobile and base-station transmit powers were fixed at 10 dBm (10 mw), i.e., no power control was used. The number of carrier frequencies in the whole system was limited to seven [12 for the fixed channel allocation (FCA) algorithm using a 12-cell cluster size], each with eight timeslots, in order to maintain an acceptable computational load. This meant that the DCA system could theoretically handle a maximum of  $7 \times 8 = 56$  (or  $12 \times 8 = 96$ ) instantaneous calls at one base station, provided that their quality was adequate. If a channel allocation request for a new call could not be satisfied immediately, it was queued for up to 5 s, after which time, if not satisfied, it was classified as blocked. It was assumed that the network was synchronous from cell to cell; thus channels on different time slots of the same frequency were orthogonal.

The physical layer was modeled using two parameters—outage SINR and reallocation SINR—defined as the average SINR required by a transceiver in order to maintain given frame error rates (FERs) over a narrow-band Rayleigh fading channel. When the signal quality, expressed in terms of the SINR, drops below the reallocation SINR, a low-quality access is encountered, and the mobile requests a new physical channel to handover to, thus initiating an intra- or intercell handover. If, while waiting for a reallocation handover, the signal quality drops further, below the outage SINR, then an outage is encountered. A prolonged outage leads to the call's being dropped or forcibly terminated. Since a user typically views a dropped call as less desirable than a blocked call, a handover queueing system (HQS) was employed. The HQS allows allocation of network resources to handovers, before assignment to new call requests, thus reducing the number of dropped calls at the expense of the blocked call probability. An additional benefit of the HQS is the time window formed, during which resource allocation may take place, thus increasing the chances of a used slot's becoming free and allowing a handover to be successfully executed. This twin-threshold physical layer model is similar to those described by Tekinay *et al.* [22] and Katzela *et al.* [23]. However, the model described here is based on SINR thresholds, rather than the received power thresholds of Tekinay *et al.* [22] and Katzela *et al.* [23]. A further metric, namely, the low-signal quality probability, is calculated as the proportion of time that the SINR is below the reallocation SINR threshold.

The outage SINR and reallocation SINR threshold were determined, via independent bit-level simulation, for BPSK, QPSK/4-QAM, and 16-QAM models, conducted in a Rayleigh fading environment using approximately half-rate Bose–Chaudhuri–Hocquenghem (BCH) codes, which employed interleaving over the different number of bits conveyed by the different modem modes. Thus, the reallocation SINR threshold was determined to be the average SINR required by the specific transceiver employed to maintain a 5% transmission FER. This SINR value is transceiver dependent and in general can be reduced at the cost of increased transceiver complexity and power consumption. The loss of a maximum of 5% of the speech or video packets can be considered a worst case scenario for modern “wireless orientated,” i.e., error-resilient source codecs. Therefore, by setting the reallocation threshold at this level, the system requested handovers to new channels before the speech or video quality degradation became objectionable.

The outage SINR threshold sets the SINR, below which the system declares that the radio channel has degraded to such a level as to cause a service outage. If the radio channel continues to be in outage, then the call is forcibly terminated. The outage SINR threshold was determined by simulations to be the average SINR required to maintain a 10% FER. Therefore, if the radio channel degrades such that at least 10% of the speech or video packets were lost for some period of time, then the call would be forcibly terminated. The SINR thresholds for BPSK, QPSK/4-QAM, and 16-QAM modems are shown in Table II.

The adaptive modulation and power control algorithm aims to minimize the probability that the SINR will drop below both the reallocation SINR and outage SINR for a given modulation mode, while also attempting to reduce the average transmission power, by determining the most appropriate combination of transmit power and modulation mode for the next transmit burst. The idea behind adaptive modulation is to select a modulation mode according to the instantaneous radio channel quality [13]. Thus, if the channel exhibits a high instantaneous SINR, then a high-order modulation mode may be employed, enabling the exploitation of the temporarily high channel capacity. Likewise, if the channel has a low SINR, using a high-order modulation mode would result in an unacceptable FER and hence a more robust but lower throughput modulation mode would be invoked. Therefore, adaptive modulation not only combats the effects of a poor quality channel but also attempts to maximize the throughput while maintaining a given target FER. Thus, there is

TABLE II

REALLOCATION SINRS AND OUTAGE SINRS USED IN THE HANDOVER PROCESS, FOUND BY SIMULATION FOR BPSK, QPSK/4-QAM, AND 16-QAM MODEMS. REALLOCATION SINR IS THE SINR BELOW WHICH A CHANNEL REALLOCATION WILL BE REQUESTED, WHILE THE OUTAGE SINR IS THE SINR, BELOW WHICH A SERVICE OUTAGE IS DECLARED. SUCCESSIVE SERVICE OUTAGES CAUSE THE CALL TO BE FORCIBLY TERMINATED

Modulation Scheme	Reallocation SINR threshold (dB) for 5% FER	Outage SINR threshold (dB) for 10% FER
BPSK	17	13
4-QAM	21	17
16-QAM	27	24

tradeoff between the mean FER and the data throughput, which is governed by the modem mode switching thresholds. These switching thresholds define the SINRs at which the channel is considered unsuitable for a given modulation mode, where an alternative mode must be invoked. The pseudocode of the proposed algorithm is as follows:

```

determine lowest SINR out of up- and down-link SINRs
if in 16 QAM mode
  if lowest SINR < 16 QAM drop SINR
    drop to 4 QAM mode
  else if lowest SINR < 16 QAM reallocation SINR
    if at maximum transmit power then revert to 4 QAM
    else increase transmit power
  else if lowest SINR < 16 QAM target SINR
    increase transmit power
  else if lowest SINR > 16 QAM target SINR + hysteresis
    decrease transmit power
else if in 4 QAM mode
  if lowest SINR < 4 QAM drop SINR
    drop to BPSK mode
  else if lowest SINR < 4 QAM reallocation SINR
    if at maximum transmit power then revert to BPSK
    else increase transmit power
  else if lowest SINR < 4 QAM target SINR
    increase transmit power
  else if lowest SINR > 16 QAM target SINR + hysteresis
    change to 16 QAM mode
  else if lowest SINR > 4 QAM target SINR + hysteresis
    if at maximum transmit power then
      reduce transmit power
    else change to 16 QAM
else if in BPSK
  if lowest SINR < BPSK drop SINR
    outage occurs
  else if lowest SINR < BPSK reallocation SINR
    if not at maximum transmit power
      then increase transmit power
  else if lowest SINR > 4 QAM target SINR + hysteresis
    change to 4 QAM
  else if lowest SINR > BPSK target_hysteresis
    if at maximum transmit power then
      reduce transmit power
    else change to 4 QAM

```

The power control and modulation mode switching algorithm invoked in our simulations attempted to minimize the transmitted power while maintaining a high throughput with a less than 5% target FER. Target SINRs of 21, 27, and 32 dB were used for the BPSK, 4-QAM, and 16-QAM modulation modes, respectively.

When simulating the network employing adaptive antennas in conjunction with adaptive modulation and power control, a multipath propagation environment was employed. This consisted of the line-of-sight (LOS) ray and two additional rays, each having a third of the power of the LOS ray, with angles of arrival at the base station determined using the geometrically-based single-bounce elliptical model (GBSBEM) of [24] and [25], with parameters chosen such that the multipath rays had one-third of the received power of the direct ray. It was assumed that all of these multipath rays arrived with zero time delay relative to the LOS path, or that a space-time equalizer [26], [27] was employed, thus making full use of the additional received signal energy. However, the many extra desired and interfering signals incident upon the antenna array rapidly consume the limited degrees of freedom of the antenna array, limiting its ability to fully cancel each source of interference.

The mobiles were capable of moving freely at a speed of 30 mi/h, in a fixed random direction and were selected at the start of the simulation from a uniform distribution within the simulation area of 49 cells, each having a radius of 218 m. However, the nonuniform traffic model limited the maximum velocity of mobile terminals within specified cells, thus creating a higher user density in these cells. This reduced mobile velocity resulted in an increased average cell crossing time, and hence higher teletraffic. For example, in Fig. 1, the mobiles occupying the gray cells all travel at 30 mi/h, while those entering the white cells have a reduced speed of 20 mi/h. The white cells therefore could be said to represent city outskirts, with the black cell being the city center, limiting the mobile speed to 9 mi/h. When a mobile leaves the simulation area, it reenters the simulation area at a random location with its speed and direction unchanged.

We investigated the algorithms both in conjunction with uniform and nonuniform traffic distributions. When the nonuniform traffic model was used, the speed of the mobiles in the central cells of the top two cell configurations in Fig. 1 was reduced. The call length and intercall time periods were Poisson distributed [10], [28] with the mean values shown in Table I. The activity rate of the users was fairly high. On average, a user would make a 60-s call every 300 s, a measure that allowed us to expedite our simulations.

Having described the simulation parameters, in the next section we present our simulation results, quantifying the amount of traffic that can be carried by each channel allocation algorithm.

## IV. PERFORMANCE STUDY

### A. Comparing the LOLIA with FCA

We commenced our investigations by comparing the FCA algorithm and the LOLIA under uniform traffic conditions. The FCA algorithm was employed with both 7- and 12-cell reuse clusters, using one carrier frequency per base station. The

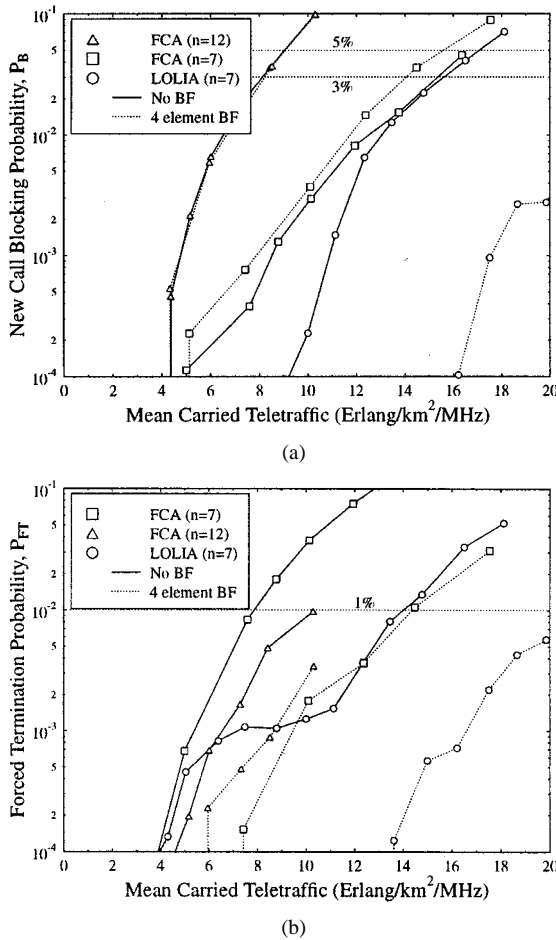


Fig. 2. (a) Call blocking and forced termination performance versus (b) mean carried traffic for comparison of the LOLIA with seven "local" base stations and FCA using 7- and 12-cell reuse clusters under uniform traffic.

LOLIA used seven nearest base stations, i.e.,  $n = 7$ , which statistically speaking has the promise of tighter channel reuse than that of the FCA scheme.

Fig. 2 shows the new call blocking and forced call termination probability for different uniform traffic loads, measured in terms of the mean normalized carried traffic expressed in Erlangs/km<sup>2</sup>/MHz. Specifically, Fig. 2(a) portrays that the FCA algorithm with a 12-cell reuse factor gives the highest new call blocking probability, followed by the FCA scheme using a seven-cell reuse factor, and then the LOLIA with the lowest probability of a blocked call. The poor blocking performance of the FCA algorithm with the 12-cell reuse factor can be attributed to its inherently poorer spectral efficiency than that of its seven-cell derivative. The lack of reduction in the new call blocking probability when using the four-element adaptive antenna arrays in conjunction with the FCA algorithms suggests that their blocking performance is limited by the available frequency/timeslot combinations. By contrast, however, the blocking performance of the LOLIA appears to be interference limited, since the addition of the adaptive antenna array results in a significantly reduced call blocking probability. Fig. 2(b) shows that the FCA algorithm using a 12-cell reuse cluster has a lower call dropping probability than that of a seven-cell reuse cluster. This is a result of the greater reuse distance between cochannel cells, leading to lower interference

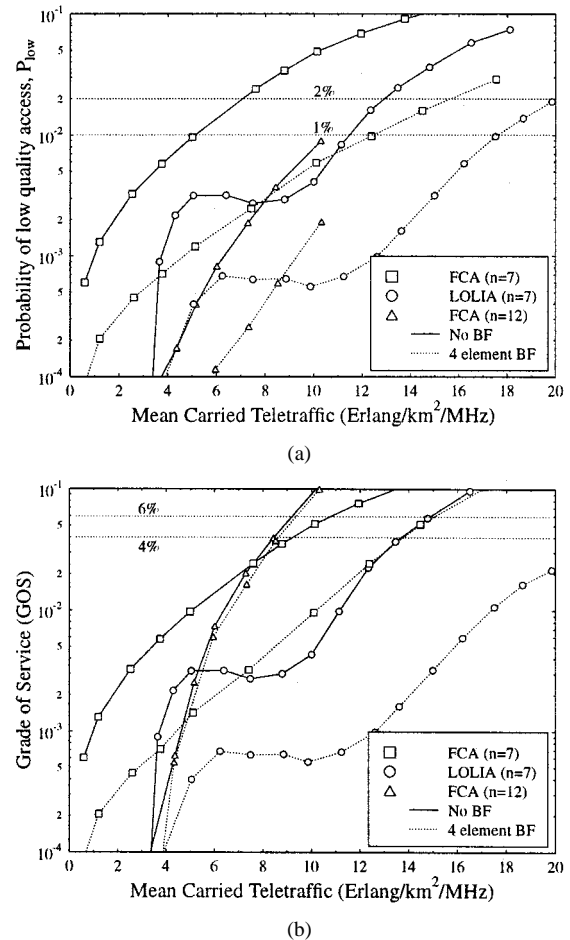


Fig. 3. (a) Probability of low-quality signal ( $P_{low}$ ) and GOS versus (b) mean carried traffic for comparison of the LOLIA with seven "local" base stations and FCA using 7- and 12-cell reuse clusters under uniform traffic.

levels and hence fewer dropped calls. The efficiency of the adaptive antenna arrays can be seen clearly in this figure, with significantly reduced call dropping probabilities observed for all of the channel allocation algorithms. It is interesting to note that the FCA algorithm with a seven-cell reuse cluster size, in conjunction with the adaptive antenna array, exhibits a lower forced termination probability than the 12-cell reuse factor variant. This is due to the greater levels of interference present with the seven-cell FCA network. Therefore, it benefits to a greater extent from the interference reduction capabilities of the adaptive antenna array.

Fig. 3 depicts the grade of service and probability of low-quality access versus a range of uniform traffic loads. It can be seen from Fig. 3(a) that the FCA algorithm using a seven-cell cluster size suffers from a significantly higher probability that low-quality access will occur. However, the FCA algorithm using a 12-cell cluster size performs much better due to its greater frequency reuse distance, reducing the interference levels. The performance of the LOLIA is superior at higher levels of teletraffic, but at lower levels it results in a greater chance of a low-quality access' occurring than for the FCA algorithm in conjunction with the 12-cell reuse factor. This results from nonoptimal channel assignments at low traffic loading due to the more dynamic nature of the traffic. By contrast, at the higher traffic loads, the system has a more

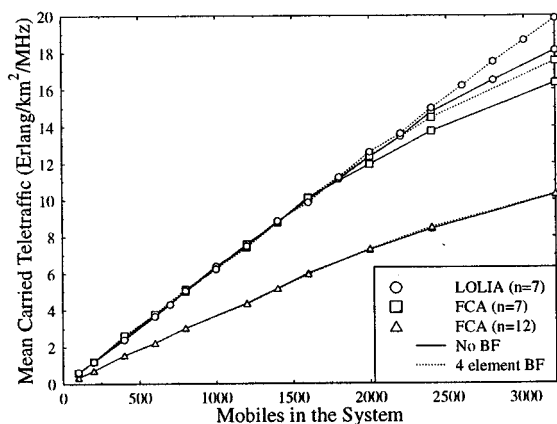


Fig. 4. Mean carried teletraffic versus number of mobile users in the system for the LOLIA with seven “local” base stations and FCA using a seven-cell reuse cluster under uniform traffic.

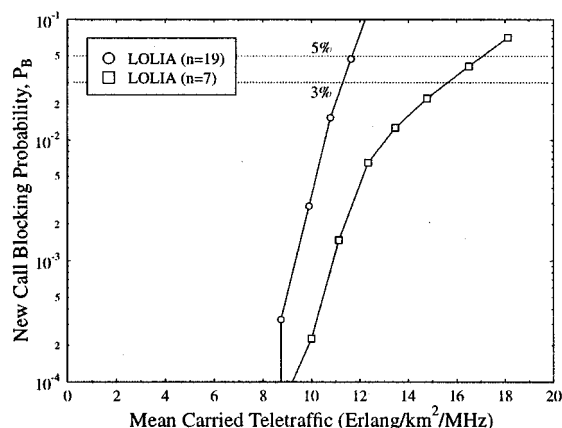
stable interference characteristic and the LOLIA can perform the channel allocations in a more beneficial manner. The GOS performance of the FCA algorithm and the 12-cell reuse factor of Fig. 3(b) are dominated by the new call blocking probability. Hence, the adaptive antenna arrays offer little reduction in the GOS. However, for both the FCA scheme using the seven-cell cluster size and the LOLIA, the performance gain of the adaptive antenna arrays is clearly evident.

Fig. 4 portrays the mean carried teletraffic versus the number of mobiles in the simulated system. The figure shows that at low traffic loads, the FCA algorithm with a seven-cell cluster size and the LOLIA carried nearly identical amounts of traffic. However, the reduced spectral efficiency of the FCA algorithm using the 12-cell cluster size is clearly evident in the figure. As the mobile density, and hence the traffic load, increased, the LOLIA carried more traffic than the FCA algorithms. It is interesting to note that the FCA algorithm with the 12-cell reuse factor does not benefit from the adaptive antenna arrays. Hence its mean carried teletraffic is dominated by the call blocking probability, and not by interference induced call dropping or low-quality access.

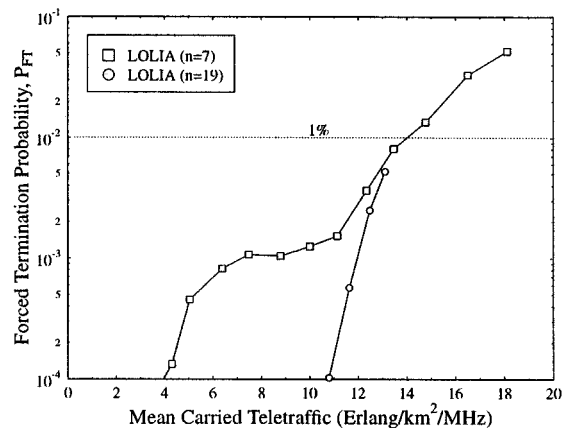
*B. Effect of the “Reuse Distance” Constraint on the LOLIA and LOMIA DCA Algorithms*

In this section, we quantify the effect of modifying the number of nearest base stations from which channel usage information is obtained when a channel allocation request is made in the LOLIA and LOMIA DCA algorithms. In the LOLIA and LOMIA, a channel cannot be allocated if it is being used in the local “neighborhood” of base stations. Therefore, by increasing the number of excluded nearest base stations in this neighborhood, the minimum reuse distance for a channel is effectively increased.

Fig. 5 displays the call blocking and forced termination probabilities for a variety of uniform traffic loads with a nearest base station constraint of seven and 19 when using the LOLIA DCA algorithm. It can be seen that the new call blocking probability is higher for the larger exclusion zone scenarios. This results from the larger exclusion zone (of 19 cells), limiting the number of available channels in the neighborhood of a user in call. Thus



(a)



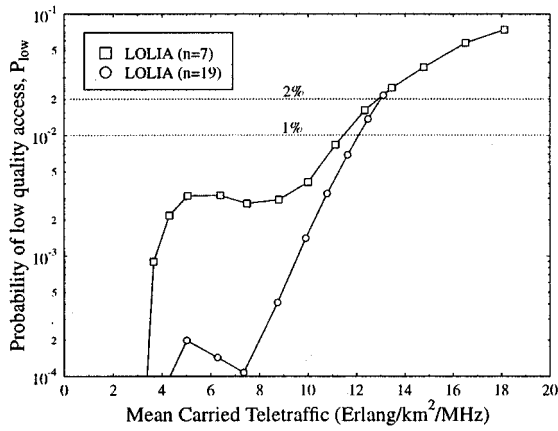
(b)

Fig. 5. (a) Blocking and forced termination performance versus (b) mean carried traffic for comparison of the LOLIA with the number of “local” base stations equal to seven and 19 under uniform traffic.

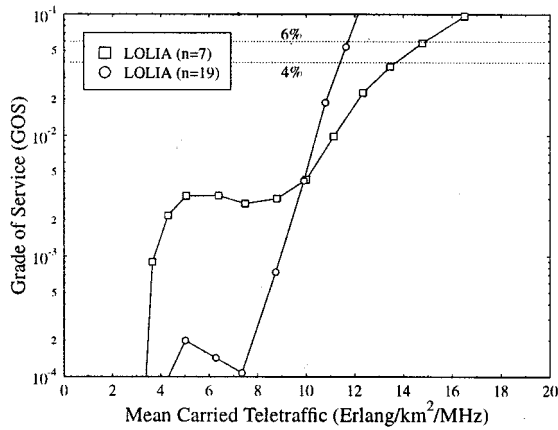
the new call blocking probability is higher. However, the use of the larger exclusion zone does reduce the forced call termination probability, especially at lower traffic loads. This is due to the increased effective reuse distance of the cochannel users, leading to a reduced level of interference and thus fewer calls dropped as a result of interference. However, at higher traffic loads, the large exclusion zone leads to resource allocation failures in the handover process and the call dropping probability degrades rapidly.

Fig. 6 shows the probability of low-quality access and the GOS for a range of uniform traffic loads, measured in terms of the carried teletraffic for the LOLIA with nearest base-station constraints of seven and 19 cells. It can be seen that the number of low-quality accesses is higher when the exclusion zone is small because the effective reuse distance is lower, inflicting more cochannel interference. The GOS is better (i.e., lower) for larger exclusion zones, when the traffic load is low, which is reversed for high traffic loads. This is mainly attributable to the higher call blocking probability of the larger exclusion zone of 19 cells, particularly in the region of the highest traffic load, as seen in Fig. 5(a).

It was found that the LOMIA required a larger exclusion zone, i.e., a higher effective reuse distance, in order to obtain similar call blocking and forced termination probabilities. This



(a)



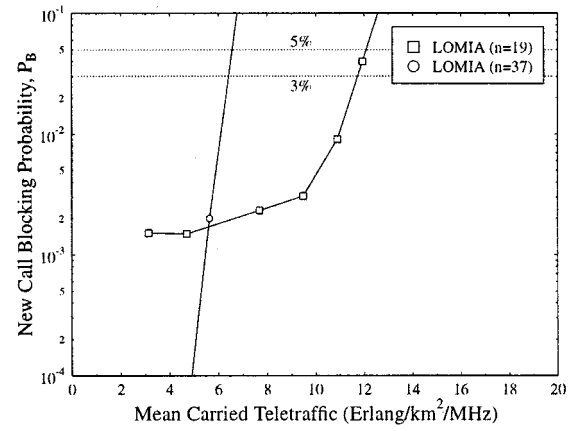
(b)

Fig. 6. (a) Probability of low-quality signal and GOS versus (b) mean carried traffic for comparison of the LOLIA with the number of “local” base stations equal to seven and 19 under uniform traffic.

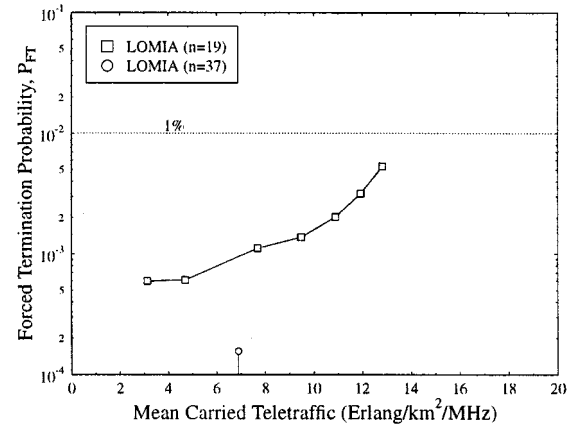
is because the LOMIA picks the most interfered channel available within the effective reuse distance. Simulations were carried out with a 19-cell exclusion zone, within a 49-cell structure, and for the LOLIA. When the exclusion zone was increased to 37 cells for the LOMIA, the number of cells in the simulation area was increased from 49 to 133 in order to enable the algorithm to configure itself properly, i.e., a 37-cell exclusion zone within a 49-cell simulation area does not give the algorithm sufficient cells to “manipulate” in order to achieve good performance.

In Fig. 7, the results are shown versus the normalized carried traffic, which is defined in terms of Erlangs/km<sup>2</sup>/MHz. Therefore, the results are independent of the size of the simulation area used for the LOMIA ( $n = 37$ ) investigations.

Explicitly, Fig. 7 shows the call blocking and forced termination probabilities versus carried teletraffic for exclusion zones of 19 and 37 cells, using the LOMIA. As expected, the LOMIA exhibits lower call blocking, but more forced terminations, when the exclusion zone is smaller. The call blocking is higher when the exclusion zone is larger since there are fewer unused channels available in the local neighborhood. The forced call termination probability is lower when the exclusion zone is larger because the effective reuse distance is larger, and hence the cochannel interference is reduced.



(a)



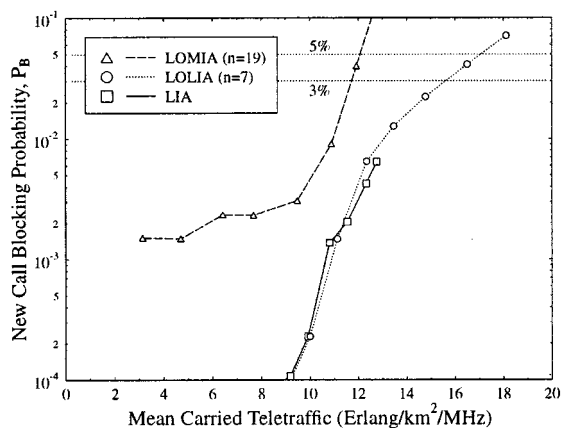
(b)

Fig. 7. (a) Blocking and forced termination performance versus (b) mean carried teletraffic for comparison of the LOMIA with the number of “local” base stations equal to 19 and to 37 under uniform traffic.

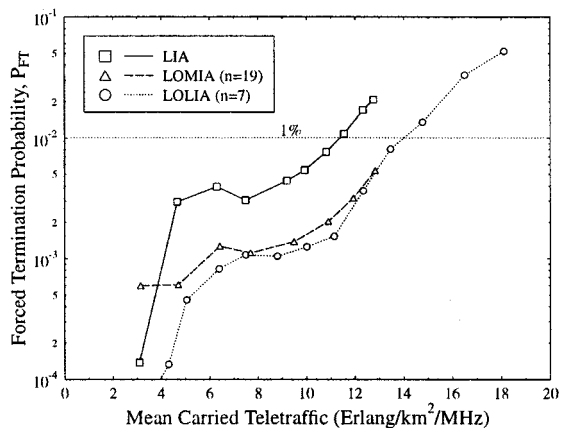
### C. Comparison of the LOLIA and LOMIA with the LIA

In this section, we compare the locally distributed DCA algorithms, LOLIA and LOMIA, with the simplest distributed DCA algorithm, the LIA. The locally distributed algorithms are expected to perform better than the corresponding distributed algorithm, since they have additional knowledge to assist in their decisions. The locally distributed algorithms are aware of the channel allocations made by the nearby base stations. However, this additional knowledge comes at the expense of additional complexity and cost required in order to signal all the channel allocations between the base stations within the neighborhood. Therefore, the LOLIA should perform better than the corresponding distributed algorithm, the LIA.

Fig. 8 shows the call blocking and forced termination probabilities versus traffic load for the LOLIA, LOMIA, and LIA DCA algorithms. The LOLIA and LIA have similar call blocking performance. However, the LIA is slightly better at higher traffic loads. This results from the LOLIAs having fewer available channels to allocate at higher traffic loads, leading to an increased call blocking probability. The LOMIA has a higher call blocking probability, i.e., lower performance, than both the LOLIA and LIA. This is due to the high reuse distance required by the LOMIA for maintaining an adequate call quality. The higher reuse distance is implemented by having



(a)



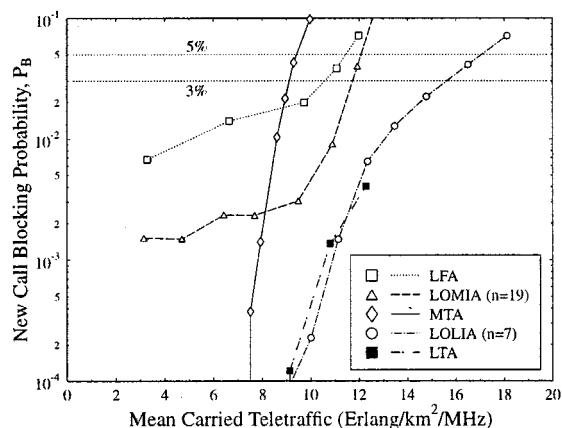
(b)

Fig. 8. Comparison of DCA algorithms: LOMIA, LOLIA, and LIA under uniform traffic. (a) New call blocking probability. (b) Forced termination probability.

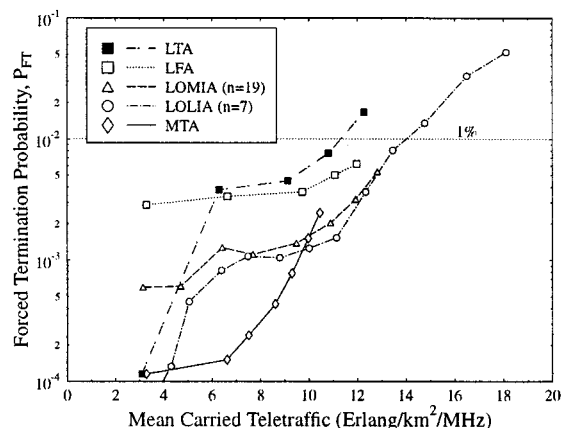
a larger exclusion zone, from which the base station receives channel allocation information. Hence, there will be fewer unused channels available, leading to the increased call blocking probability. The figure also shows that, both the LOMIA and LOLIA achieve lower forced call termination probabilities than the LIA. This is because the interference is more easily controlled in the LOLIA and LOMIA by the exclusion zone constraint. It should be noted that the LOLIA achieves a better call termination performance than the LOMIA.

#### D. Interference Threshold-Based Distributed DCA Algorithms

Interference threshold-based DCA algorithms rely on an interference threshold in order to maintain the minimum required signal quality. An interference threshold-based channel allocation algorithm will not allocate a channel if the measured interference in that channel is higher than the maximum tolerable interference threshold. The interference threshold must be above the noise floor, otherwise no channel can be allocated. The closer the interference threshold is to the noise floor, the less the interference in the system. Increasing the interference threshold allows more interfered channels to be allocated to channel requests. The effective reuse distance of the interference threshold-based DCA algorithms is dependent on the interference threshold. As the interference threshold is increased,



(a)



(b)

Fig. 9. Comparison of interference threshold-based distributed DCA algorithms (LTA, MTA, LFA) with locally distributed DCA algorithms (LOLIA, LOMIA) using a uniform traffic distribution. (a) New call blocking probability. (b) Forced termination probability.

the effective reuse distance is decreased, allowing more calls to be handled at the expense of higher interference.

We found that the optimal interference threshold for the LTA, MTA, and LFA algorithms was extremely sensitive to traffic loads and propagation conditions. This meant that the interference threshold would need to be adaptable to changing conditions. This would render the interference threshold-based distributed DCA algorithms more complex. The threshold-based algorithms require two interference thresholds: one for admitting new calls and one for handovers of calls in progress. Generally the interference threshold is adjusted to give a higher priority to handovers than to new calls, which is another form of handover prioritization. A range of interference thresholds were investigated for the three interference threshold-based algorithms—namely, for the LTA, MTA, and LFA—using various traffic loads in order to find the optimal threshold values. To simplify the optimization process, the difference between the handover and new call interference threshold was fixed at 5 dB.

Fig. 9 shows the new call blocking and forced termination probabilities versus traffic load for the above three interference-based distributed DCA algorithms, the LTA, LFA, and MTA, and for the two locally distributed algorithms, the LOLIA and LOMIA. The LTA and LOLIA have the best new call blocking performance, a consequence of their interference minimization



techniques. More specifically, if the interference level is above the maximum tolerable interference threshold, calls are blocked. Therefore, by reducing the interference in the system, more successful channel allocations may be performed. The MTA has the highest probability of a blocked call, resulting from its attempts to allocate the most interfered channel available, having an interference level below the acceptable interference threshold. When the traffic load is low, there are many unused channels, which exhibit an interference level below the interference threshold, and these are allocated to requests by the MTA. However, at high traffic loads there is a high amount of interference present in the system, and hence few channels are classed as suitable for allocation, leading to a high probability of a blocked call. Therefore, at low traffic loads, a very low new call blocking probability is achieved by the MTA, but at high traffic loads, its blocking performance is extremely poor. The blocking performance of the LFA is also poor due to its attempts to utilize the minimum number of carrier frequencies.

Fig. 9(b) shows the forced termination probability versus traffic load. Comparing these call dropping results in this figure with the call blocking results of Fig. 9(a) shows that generally, a channel allocation algorithm exhibits either a low new call blocking probability or a low call dropping probability. The LTA and MTA exemplify this, with their “complemented” performance characteristics. However, the flexibility of the locally distributed DCA algorithms, the LOLIA and the LOMIA, allows them to trade off the two performance measures and thus to provide both the lowest new call blocking probability and the lowest call dropping probability.

#### E. Performance Comparison of Fixed and DCA Algorithms Using Nonuniform Traffic Distributions

In order to show the performance benefits of DCA under nonuniform traffic conditions, we investigated the performance of FCA and some DCA algorithms using the nonuniform traffic model described in Section III-C. We decided to have a “hotspot” cell, surrounded by some less heavily loaded cells for our nonuniform traffic distribution. This is shown in Fig. 1, where the black cell in the center is the most heavily loaded cell, since mobile terminals are limited to a maximum speed of 4 m/s (9 mi/h). The black “hot spot” cell is surrounded by six white “warm spot” cells, in which the maximum mobile speed is limited to 9 m/s (20 mi/h). All the other cells (gray) serve mobile terminals that move with a constant velocity of 13.4 m/s (30 mi/h). The effect of these “hot spot” cells is that mobile terminals stay longer in such cells, increasing the terminal density and hence the teletraffic.

Another way of showing the benefits of DCA algorithms over FCA under nonuniform traffic conditions is to study the probability density function (pdf) of instantaneous traffic at a range of basestations. Fig. 10 shows the pdf of instantaneous traffic measured in Erlangs at several base stations using both uniform and nonuniform traffic distributions for fixed and DCA algorithms. Under a nonuniform traffic distribution, the figure shows the histogram of the number of channels used at each of the three types: [normal (30 mi/h), warm spot (9 mi/h), and hot spot (4 mi/h)] of cell. The FCA algorithm is limited to a maximum of eight instantaneous calls (8 erlangs), since each base station has only

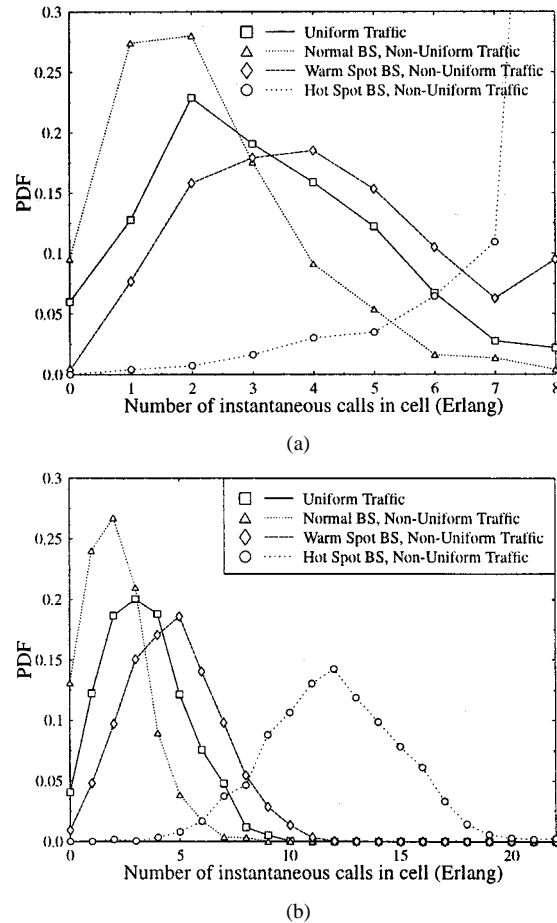
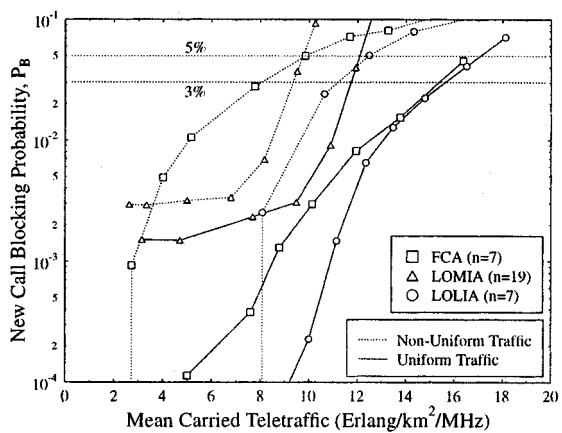


Fig. 10. PDF of the number of instantaneous calls at a basestation in terms of erlangs for uniform traffic and for the three possible cell types in nonuniform traffic. Results are shown for (a) the FCA algorithm and (b) the LOLIA with  $n = 7$ .

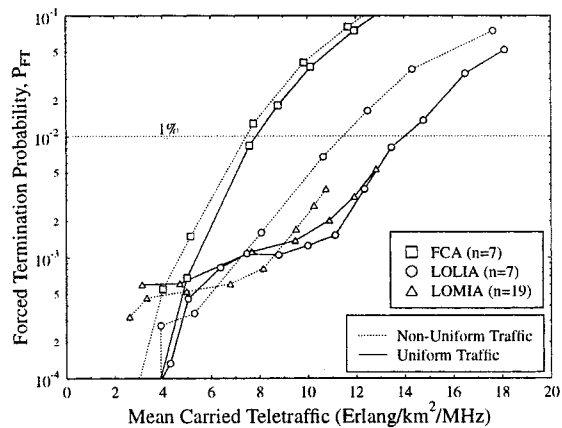
one carrier frequency and eight timeslots. This is clearly shown by the pdf of the “hot spot” cells, where, for 81% of the time, all eight channels are in use simultaneously. However, the dynamic nature of the LOLIA allows it to theoretically support 56 calls simultaneously on one base station, albeit with no calls on the surrounding  $n$  base stations. Thus, the LOLIA can support many more simultaneous calls on a base station than the FCA algorithm, as shown in Fig. 10(b), where the “hot spot” cell carried in excess of 20 erlangs under nonuniform traffic conditions. Clearly, these results have shown the benefits of DCA in terms of being able to cope with unexpected peaks of traffic demand.

These results have shown that the LOLIAs can carry more teletraffic than the FCA algorithm when the traffic distribution is nonuniform. However, we will now show how the performance of the various channel allocation algorithms changes, in comparison to our previous results throughout Section IV, when subjected to nonuniform traffic distributions.

Fig. 11 portrays the new call blocking and call dropping probabilities of the FCA algorithm, the LOLIA, and the LOMIA under uniform and nonuniform traffic distributions. The FCA algorithm suffered the greatest degradation in call blocking performance in nonuniform traffic conditions. Specifically, due to its FCA, each cell was limited to one carrier frequency regardless of its traffic load, hence leading to high call blocking in



(a)



(b)

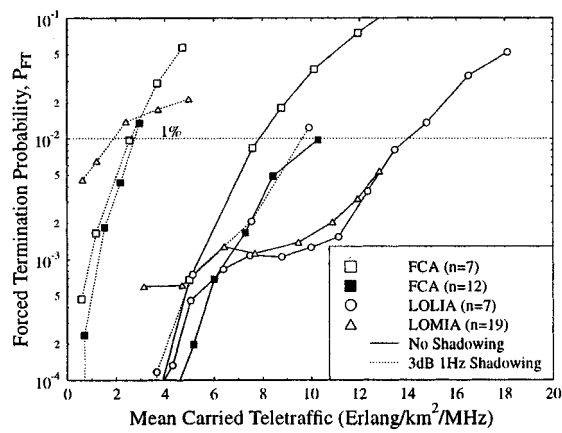
Fig. 11. (a) Blocking and forced termination performance versus (b) mean carried traffic for comparison of the LOLIA, LOMIA, and FCA under both uniform and nonuniform traffic distributions.

cells with a high user density. However, since the LOLIA and the LOMIA are part of the family of DCA algorithms, they are capable of sharing channels between cells, subject to the exclusion zone constraints, and consequently suffer less performance degradation than the FCA algorithm.

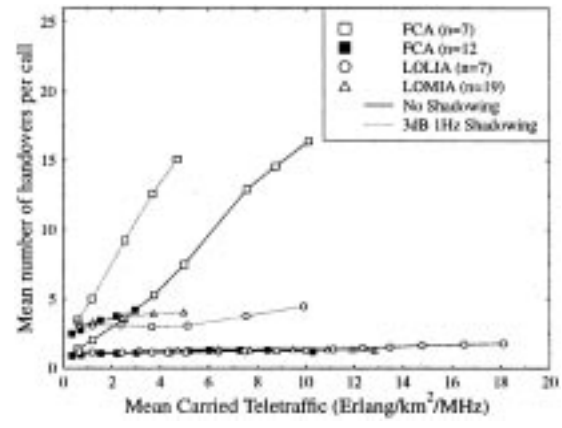
The comparison of the forced termination probability under uniform and nonuniform traffic loading is shown in Fig. 11(b). The FCA algorithm suffered only a small increase in the dropped call probability, which was most likely limited by the HQS' giving priority to handovers at the expense of new call requests, as can be clearly seen in Fig. 11(a). The LOLIA and the LOMIA also suffer a performance gradation in the nonuniform traffic conditions, which becomes more evident as traffic levels increase. At low levels of traffic, it is possible for the channel allocation algorithms to allocate sufficient resources to the cells with the highest user densities while maintaining the coverage of the other, lower traffic cells and meeting the exclusion zone constraints. However, at higher traffic levels, the exclusion zone renders the frequency reuse to be limited, and hence calls are dropped due to a lack of network resources.

*F. Effect of Shadow Fading on the FCA, LOLIA, and LOMIA*

In this section, we quantify the effect of shadow fading on three channel allocation algorithms. For our shadow fading in-



(a)



(b)

Fig. 12. (a) Forced termination performance and mean number of handovers performed per call versus (b) mean carried traffic for comparison of the LOLIA, LOMIA, and FCA algorithm with and without shadowing. Log-normal shadow fading was generated with a frequency of 1 Hz and a standard deviation of 3 dB.

vestigations, we used a log-normally distributed shadow fading model, with a fading frequency of 1 Hz and a standard deviation of 3 dB. We performed simulations with and without shadow fading using the FCA algorithm and the two locally distributed DCA algorithms, LOLIA and LOMIA.

Fig. 12(a) shows the forced termination probability versus mean carried teletraffic with and without shadow fading (standard deviation = 3.0 dB, frequency = 1.0 Hz) for the FCA algorithm, the LOLIA, and the LOMIA. As expected, the forced termination was higher for all traffic loads when the propagation environment included shadow fading. The FCA algorithm demonstrated the worst forced termination probability both with and without shadowing except at the lowest traffic loads, where, despite its larger "exclusion zone" of 19 base stations, the LOMIA exhibited the worst forced termination probability due to its allocation of the most interfered channels. The lowest forced termination probability was obtained using the LOLIA, regardless of whether shadow fading was used or not. The reduced performance of these channel allocation algorithms in the shadow-fading environment can be attributed to the more rapidly changing interference levels of the network.

In Fig. 12(b), the mean number of handovers per call is plotted against the mean carried teletraffic. The figure shows that the FCA algorithm in conjunction with the seven-cell

cluster size performs significantly more handovers than all the other channel allocation algorithms, including the FCA algorithm using a 12-cell cluster size. This suggests that the performance of the FCA algorithm with the seven-cell cluster size is limited by the interference arising from its smaller reuse distance. However, the FCA algorithm using a 12-cell cluster size leads to reduced levels of interference, and hence the number of handovers performed per call is significantly lower, as exemplified by Fig. 12(b). When the radio channels are shadow-faded, the LOLIA performs the lowest number of handovers, which is a consequence of allocating the least interfered channels that are likely to withstand the irregular channel impairments of shadowed channels. For both non-shadow-faded and shadow-faded radio channels, the FCA algorithm employing a seven-cell reuse cluster performed the greatest number of handovers. By contrast, in conjunction with a 12-cell reuse cluster, the FCA algorithm performed well, given its simplicity. These results show that the performance of all of the channel allocation algorithms is severely affected by shadow fading. However, the DCA algorithms, particularly the LOLIA, cope best with the channel degradation caused by shadow fading. In the next section, we study the effect of the shadow-fading frequency and standard deviation on the LOLIA.

#### G. Effect of Shadow Fading Frequency and Standard Deviation on the LOLIA

In this section, we investigate the performance effects of the LOLIA among different shadow-fading conditions. We investigated the LOLIA using a seven-cell exclusion zone ( $n = 7$ ) and 1400 users employing QPSK modulation for a range of shadow-fading frequencies and standard deviations. The shadow-fading frequencies investigated were 0.25, 0.5, 1.0, and 2.0 Hz. The standard deviation of the shadow fading was varied from 1.0 to 12.0 dB.

The forced termination probability is plotted versus the standard deviation of the shadow fading for the range of shadow-fading frequencies in Fig. 13(a). The figure shows the expected increase of the forced termination probability as either the standard deviation or the fading frequency of the shadow fading increases.

Fig. 13(b) shows the mean carried teletraffic plotted versus the standard deviation of the shadow fading for the range of shadow-fading frequencies. The figure illustrates that the carried teletraffic rolls off more rapidly, as the standard deviation increases, for faster fading rates. The reduction in carried teletraffic, as the fading standard deviation is increased, is due to the wider power range over which the shadow fading may vary the received signal power. Hence, larger changes in the interference levels are inflicted upon other users, causing calls to be forcibly terminated and eventually reducing the carried teletraffic. The carried teletraffic performance is worse at higher shadow-fading frequencies, as observed for the forced termination performance earlier.

Fig. 14 shows the average number of handovers per call and the grade of service for a range of shadow-fading frequencies and fading standard deviations in the context of the LOLIA.

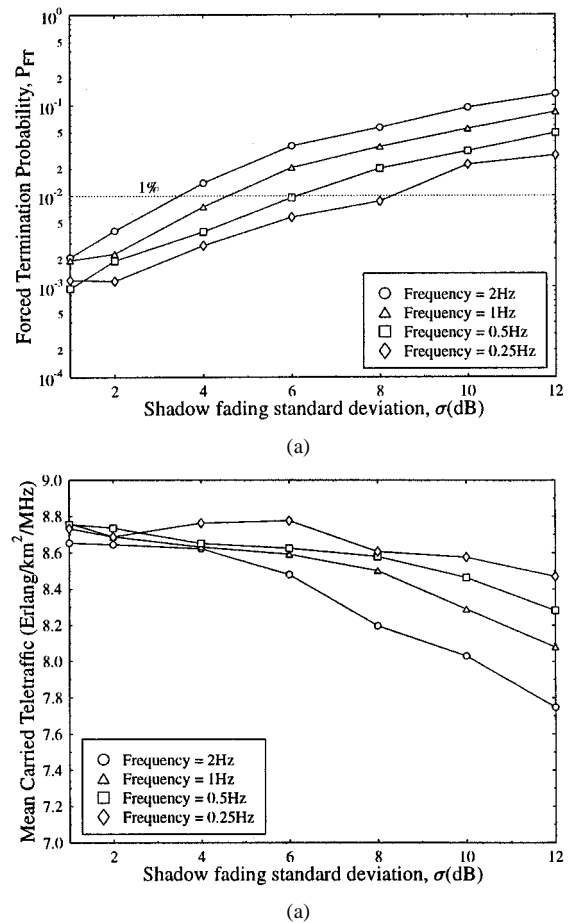
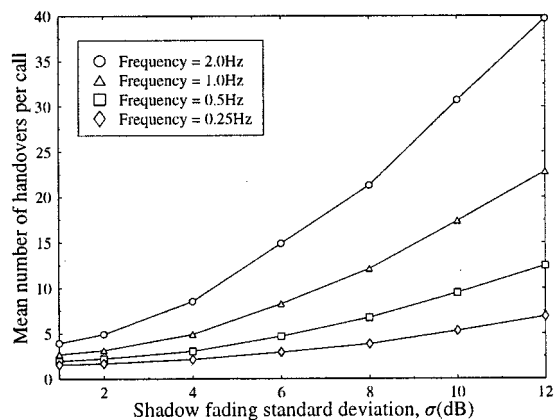


Fig. 13. (a) Forced termination performance and mean carried traffic versus (b) shadow fading standard deviation and frequency, using the LOLIA with an exclusion zone of seven cells ( $n = 7$ ). A total of 1400 mobile users were simulated in a 49-cell area, all using the 4-QAM/QPSK modulation scheme.

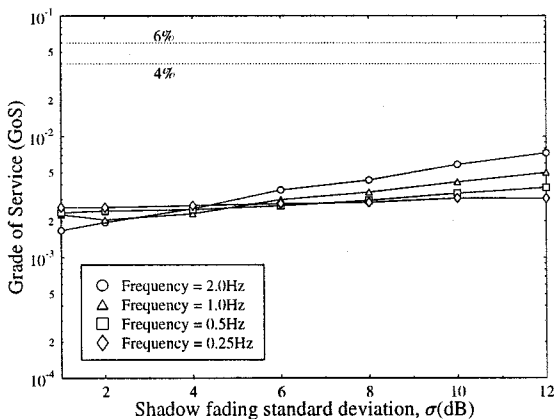
The average number of handovers per call is shown to increase with the standard deviation and frequency of the shadow fading. Every time a handover is required, either because of moving between cells or due to increased interference, the chance of the call's being forcibly terminated increases. Therefore, it is wise to restrict handovers to those calls that are most likely to succeed.

The figure shows that the number of handovers increases with both the frequency and the standard deviation of the shadow fading. However, it is at the higher fading frequencies that the variation of the standard deviation has the most pronounced effect, with a ten-fold increase in the number of handovers performed upon increasing the standard deviation from 1.0 to 12.0 dB at a fading frequency of 2 Hz. At a fading frequency of 0.25 Hz, an increase by slightly less than a factor of 4.5 was observed under the same conditions. Hence, the combination of received signals and interfering signals varying rapidly over a wider range of powers leads to handovers' being performed more frequently.

Fig. 14(b) shows the grade of service for a range of shadow-fading frequencies and standard deviations. The grade of service is superior (i.e., lower) for the higher fading frequencies, when the fading standard deviation is below about 4 dB. Above this point, the faster fading frequencies offer a poorer grade



(a)



(b)

Fig. 14. (a) Average number of handovers per call and the GOS versus (b) shadow-fading standard deviation and frequency. The LOLIA with an exclusion zone of seven cells ( $n = 7$ ) was used. A total of 1400 mobile users were simulated in a 49-cell simulation area, all using the 4-QAM/QPSK modulation scheme.

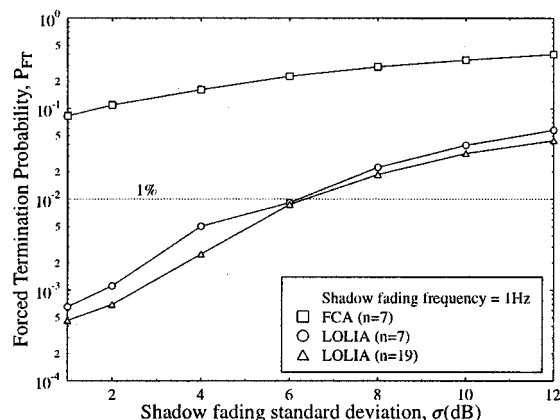
of service (i.e., increased). This is due to the combination of the higher fading frequencies and lower standard deviations, leading to shorter periods of time during which the received signal quality is poor, and hence low-quality accesses. However, at higher standard deviations, the variation of the received signal quality is significantly higher, and the increased fading frequency leads to a greater likelihood of a poor-quality access. In the next section, we investigate the effect of the standard deviation of the shadow fading on the FCA algorithm and the LOLIA.

*H. Effect of Shadow Fading Standard Deviation on FCA and LOLIA*

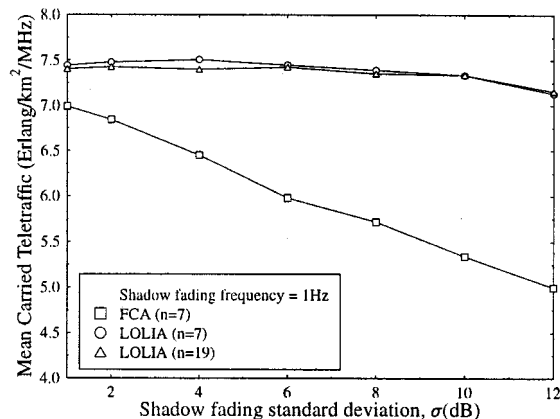
In this section, we study the effect of shadow fading on both fixed and DCA algorithms employed in a 49-cell network supporting 1200 users. We employed an FCA scheme with a seven-cell reuse cluster and the LOLIA using exclusion zones of both seven and 19 cells.

Fig. 15 shows the forced termination and carried traffic performance versus the standard deviation of the shadow fading for FCA and LOLIA in conjunction with  $n = 7$  and 19.

As the shadow-fading standard deviation increases, so does the range over which the desired signal power and the unde-



(a)



(b)

Fig. 15. (a) Forced termination probability and mean carried traffic versus (b) shadow fading standard deviation. Simulations use the LOLIA, with an exclusion zone of seven and 19 cells ( $n = 7$  and 19), and FCA ( $n = 7$ ). A total of 1200 mobile users were simulated in a 49-cell simulation area, all using 4-QAM/QPSK modulation thresholds.

sired interference power may vary. Hence, as the shadow-fading standard deviation increases, the received signal-to-interference ratio varies over a wider range at a higher rate of change. Furthermore, the chance of a handover to base stations that are not geographically the closest ones becomes more likely. Handovers to a base station when the mobile is not in that cell’s designed coverage area are not a problem in the context of DCA algorithms, since they can adapt. However, such handovers can spuriously reduce the designed reuse distance in FCA.

Fig. 15(a) shows the forced termination probability for the three channel allocation algorithms—namely, for FCA and for LOLIA using  $n = 7$  and 19. As expected, FCA is outperformed by the DCA algorithms. Furthermore, the LOLIA algorithm with the more stringent reuse distance constraint ( $n = 19$ ) performs better than the LOLIA with an exclusion zone of  $n = 7$ . Although not shown in the figure, the FCA simulations exhibit a marked increase in the number of intracell handovers, or handovers within the same cell. This is a sign of the interference’s causing call outages and requesting an emergency intracell handover.

The high forced termination probability of the FCA algorithm causes a drastic reduction in carried traffic, as shown in Fig. 15(b). The figure shows that the carried traffic using the FCA algorithm is lower than that of either of the  $n = 7$  and

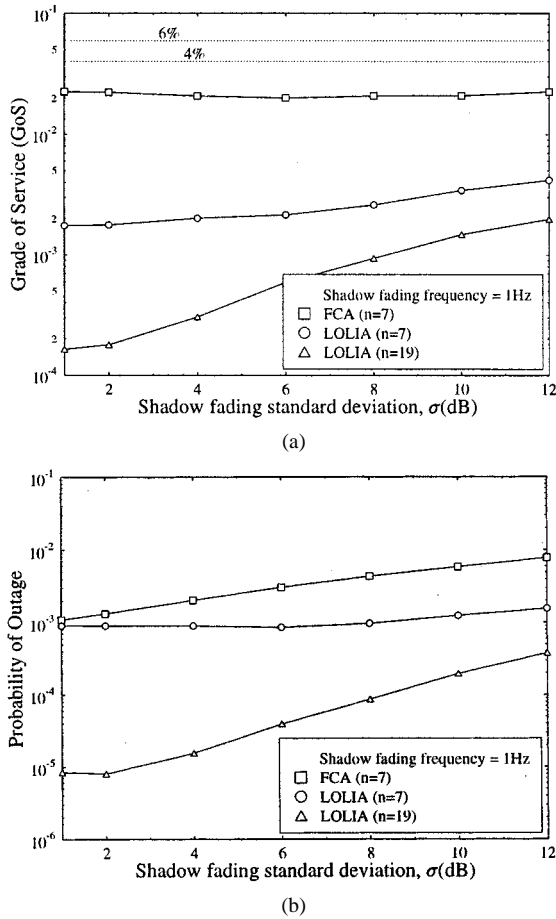


Fig. 16. (a) GOS performance and probability of outage versus (b) shadow-fading standard deviation. Simulations use the LOLIA with an exclusion zone of seven and 19 cells ( $n = 7$  and 19), and FCA ( $n = 7$ ). A total of 1200 mobile users were simulated in a 49-cell simulation area, all using the 4-QAM/QPSK modulation scheme.

19 LOLIAs, and the level of traffic carried decreases the most rapidly as the shadow-fading standard deviation is increased. The carried traffic upon using the LOLIAs remains nearly constant until a standard deviation of about 10 dB is reached, at which point a noticeable change of gradient occurs.

Fig. 16 displays various GOS performance metrics. The grade of service is the probability that a new call is blocked, or, if the call attempt is successful, that the quality of the channel provided is poor, which is shown in Fig. 16(a). The figure demonstrates that the LOLIAs consistently provide a better (lower) grade of service than the FCA algorithm. The increased reuse distance of the LOLIA with  $n = 19$  results in a significantly lower grade of service than that of the LOLIA using an exclusion zone of seven cells. The FCA algorithm, with its fixed seven-cell reuse cluster size, exhibits the poorest performance, which remained approximately constant for all of the shadow-fading standard deviation values, a side-effect of the high rate of dropped calls. In other words, the number of low-quality accesses is limited because the calls are frequently dropped once a low-quality access has occurred.

The probability of outage, which was defined in Section III-A, is shown in Fig. 16(b). Again, the LOLIA with  $n = 19$  offers the best performance, followed by the LOLIA using  $n = 7$  and, lastly, the FCA algorithm using a seven-cell

reuse cluster size. In the next section, we analyze the distribution of the SINR profiles across the cells.

### I. SINR Profile Across Cell Area

In addition to the performance metrics we derived in Section III-A, our mobile radio simulator can provide a range of other statistical characteristics, such as the signal quality across the simulation area. The simulator divides the service area into a fine grid, and for every time interval when a mobile is in a specific grid square, the statistics for that grid square are updated. For each grid square, the minimum, maximum, and average values for the SIR, SINR, SNR, and the interference signal strength are recorded. In this section, we compare the uplink SINR profiles of the FCA algorithm and the LOLIA. For the LOLIA, we used an exclusion zone of 19 cells ( $n = 19$ ). This LOLIA setup uses information from the 19 nearest basestations and hence has approximately the same reuse distance as the FCA algorithm employing a seven-cell reuse cluster. However, in highly loaded situations, the number of interferers that are approximately the reuse distance away from the user could be far higher for the LOLIA than the limit of six in the case of the FCA algorithm.

Fig. 17 shows the minimum uplink SINR profile across the cell, which identifies the areas where the minimum SINR is very low. These are the areas where outages are more likely to occur. The figure shows that the minimum SINR is less predictable for the LOLIA, since the contours are not as smooth as for FCA; and the three-dimensional view is less defined than for the FCA algorithm. However, the LOLIA achieves a higher minimum SINR than the FCA algorithm, as evidenced by the contour plots in Fig. 17(b) and (d). In these figures, the contours are at 5-dB intervals, with every 20-dB interval being labeled. The 40-dB contours are so small that they are not labeled in the FCA results shown in Fig. 17(b), whereas the 40-dB contour area is considerably larger for the LOLIA, as characterized in Fig. 17(d). Furthermore, the 20-dB contour is more erratic in the LOLIA simulations but is farther from the base stations, indicating a better signal quality between the base stations than for FCA.

The results in this section have demonstrated that the LOLIA achieves better SINR performance across the cell area than the FCA algorithm. In the next section, we attempt to combine the different performance metrics in order to produce an overall comparison between the various channel allocation algorithms that we have investigated.

### J. Performance of the Adaptive Modulation Scheme Using Power Control and Adaptive Antennas over a Multipath Channel

Fig. 18(a) shows the new call blocking probability versus the mean normalized carried traffic. From this figure, it can be seen that in conjunction with the LOLIA, there are no blocked calls except for at the highest level of traffic when using a two-element antenna array. However, in general, the FCA algorithm exhibited a higher blocked call probability. This was a direct consequence of the reduced call dropping probability's leading to a higher load on the network's resources and, hence, fewer new calls were allocated to these resources.

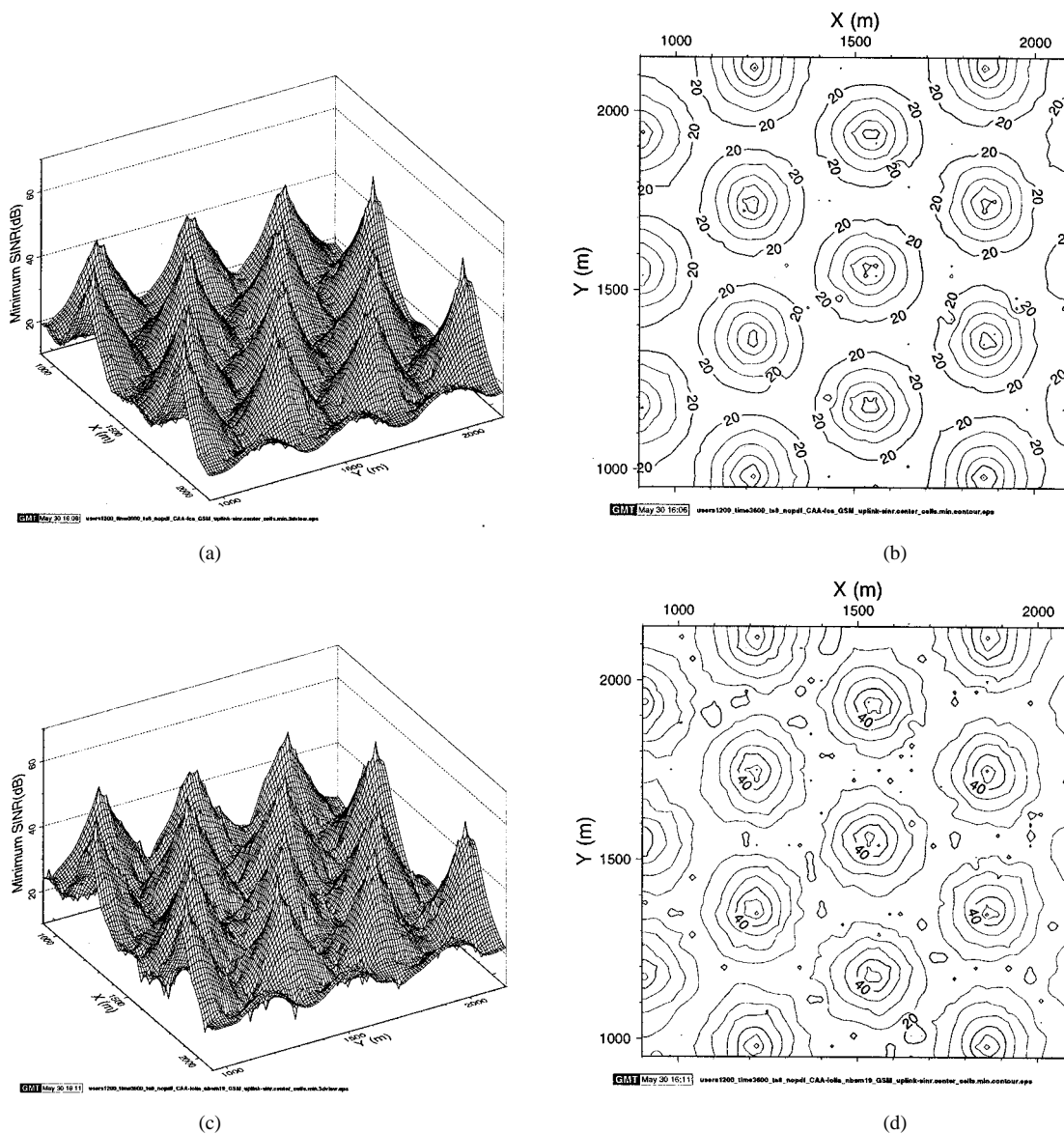


Fig. 17. Minimum uplink SINR profile across the experimental area for several cells in the center of a 49-cell simulation. The results correspond to 1200 4-QAM/QPSK mobiles under uniform traffic distribution and without shadow fading, using FCA in conjunction with a seven-cell cluster size and the LOLIA using  $n = 19$ . The contour lines are 5 dB apart. (a) FCA  $n = 7$  (3-D view). (b) FCA  $n = 7$  (contour view). (c) LOLIA  $n = 7$  (3-D view). (d) LOLIA  $n = 7$  (contour view).

The call dropping probability, depicted in Fig. 18(b), shows that when invoking adaptive modulation, the FCA algorithm performs better than the LOLIA below a traffic load of about 32 erlangs/km<sup>2</sup>/MHz. The FCA scheme consistently offered a lower call dropping probability when employing adaptive quadrature amplitude modulation (AQAM) than when using the 4-QAM modulation mode. However, the AQAM-assisted LOLIA using a two-element adaptive antenna array performed slightly worse than 4-QAM for traffic levels below about 30 erlangs/km<sup>2</sup>/MHz. Nonetheless, above this level, the LOLIA performance remained relatively constant, whereas for 4-QAM, the dropping probability increased fairly sharply.

From Fig. 19(a), it can be seen that the GOS of the FCA algorithm did not benefit from AQAM to the same extent as the LOLIA. The FCA scheme using AQAM and a two-element antenna array offered a marginally lower, i.e., better GOS than fixed 4-QAM combined with a four-element antenna array. Con-

versely, the GOS of the LOLIA was reduced by up to a factor of 200 at a traffic load of about 40 erlangs/km<sup>2</sup>/MHz. Above this load, the GOS increased steeply due to the nonzero blocking probability incurred under this traffic loading.

Fig. 19(b) shows that the probability of a low-quality access was reduced due to AQAM for both the FCA scheme and the LOLIA. For traffic loads below about 10 erlangs/km<sup>2</sup>/MHz, the FCA algorithm using AQAM behaved similarly to fixed 4-QAM, but when more moderate levels of traffic were reached, the advantage of adaptive modulation increased. Likewise, for low traffic levels, the LOLIA gained little from investing in AQAM, but for higher traffic loading, the probability of a low-quality access' occurring levelled off to a near constant value.

The average modem throughput expressed in bits per symbol versus the mean carried teletraffic is shown in Fig. 20(a). The figure shows how the mean number of bits per symbol decreased as the network traffic increased. The FCA algorithm offered the

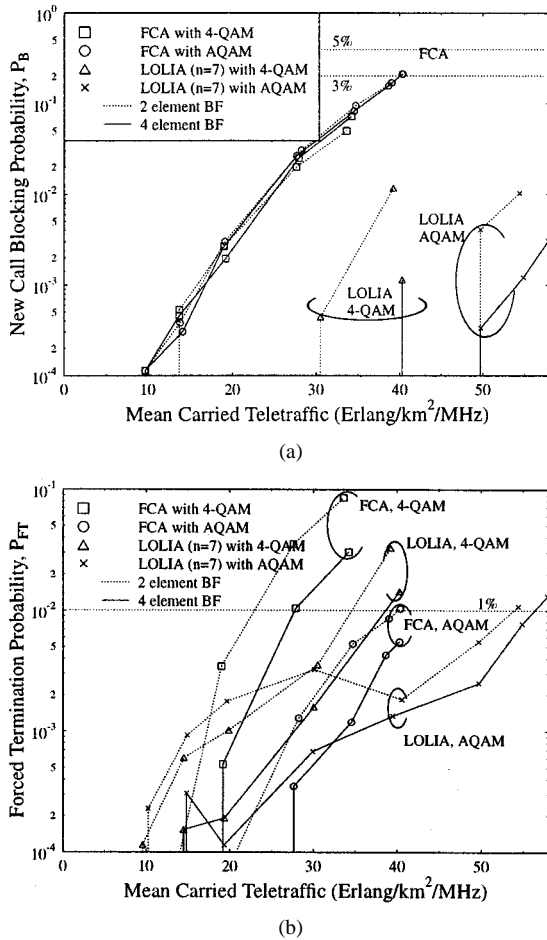


Fig. 18. (a) New call blocking and call dropping probabilities versus (b) mean carried traffic of the LOLIA using  $n = 7$ , and of FCA employing a seven-cell reuse cluster, for LOLIA using two- and four-element antenna arrays, with and without adaptive modulation.

least throughput, with its performance degrading near linearly with increasing network traffic. The LOLIA, especially for the lower levels of traffic, offered a higher modem throughput for a given level of teletraffic carried, with the performance gracefully decreasing as the carried teletraffic continued to increase.

The mean transmission power results of Fig. 20(b) demonstrate how the employment of AQAM can reduce the power transmitted for both the up- and the downlink. At low traffic levels, the FCA algorithm performed noticeably worse in transmitted power terms than the LOLIA. However, as the traffic loads increased, the difference became negligible. By contrast, the gap between the up- and the downlink powers was close to zero for the lighter traffic loads, but as the level of network traffic increased, so did the difference, with 2 dB extra transmit power required on the uplink for the maximum traffic load simulated. This resulted from the interfering mobiles' being located closer to the serving base station than the interfering base stations are to the served mobile. The mean power reduction, when compared to a fixed transmission power of 10 dBm, varied from approximately 1 to more than 8 dB. A 1-dB reduction in transmission power is not particularly significant for the mobile user, especially since at this network load, a throughput of just 2 bits/symbol is possible. The difference between the network using adaptive modulation and that without, though, is the

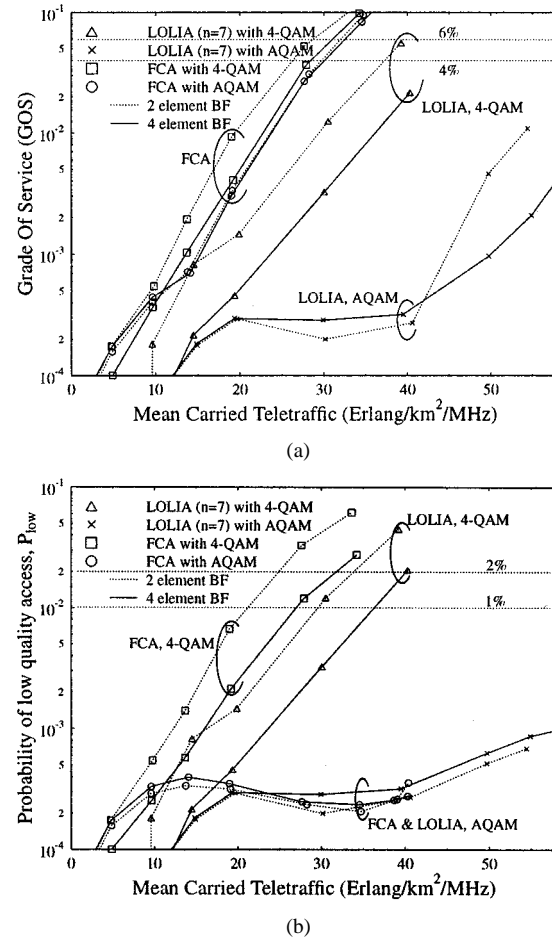


Fig. 19. (a) GOS and probability of a low-quality outage versus (b) mean carried traffic of the LOLIA using  $n = 7$ , and of FCA employing a seven-cell reuse cluster, for two- and four-element antenna arrays with and without adaptive modulation.

overall improved call quality that can be achieved in these circumstances.

### K. Overview of Results

In our previous investigations, we have simulated several channel allocation algorithms. However, no single algorithm performs best in terms of every performance metric. Therefore, in order to compare our results for the fixed and the various DCA algorithms, it is necessary to consider a combination of performance metrics. Sometimes an algorithm may provide excellent performance in terms of one metric but poor performance in terms of another. Therefore, we defined a conservative and a lenient scenario as follows:

- 1) a *conservative scenario*, where the maximum acceptable value for the new call blocking probability  $P_B$  is 3%, for the forced termination probability  $P_{FT}$  is 1%, for  $P_{low}$  is 1%, and for the GOS is 4%.
- 2) a *lenient scenario*, in which the forced termination probability  $P_{FT}$  still must be less than 1% but the maximum tolerable percentage for the blocking probability  $P_B$  is 5%, for  $P_{low}$  is 2%, and for the GOS is 6%.

For the network employing adaptive modulation techniques, a further restriction of a minimum mean modem data throughput of 2 bits/s was applied.

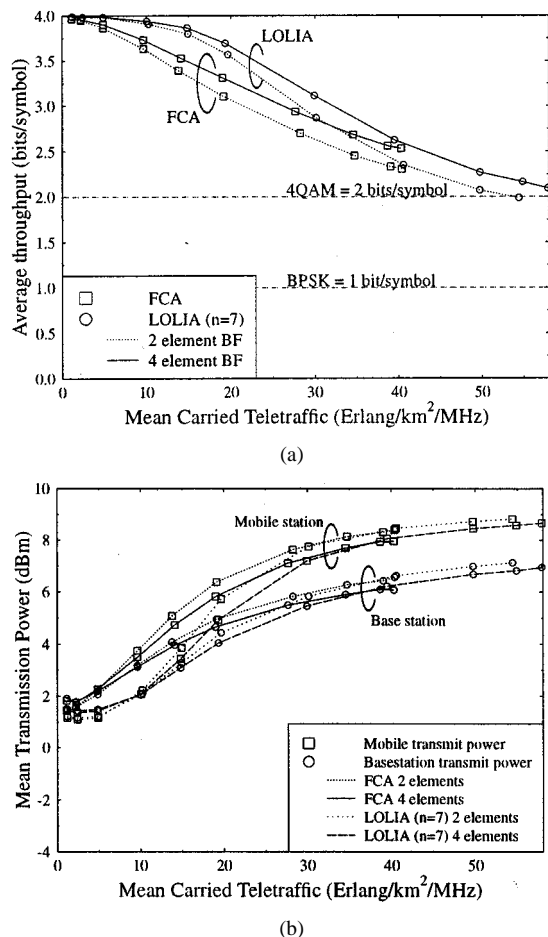


Fig. 20. (a) Mean modem throughput in terms of bits per symbol and mean transmit power versus (b) mean carried traffic of the LOLIA using  $n = 7$ , and of FCA employing a seven-cell reuse cluster, for two- and four-element antenna arrays with adaptive modulation. Without adaptive modulation, mean throughput was 2 b/s and mean transmit power was +10 dB.

The maximum traffic load, measured in terms of the number of users in the system that could be served while maintaining the constraints imposed by the above two scenarios, is shown in Table III, portraying results for both uniform and nonuniform traffic distributions. The number of users in the table is distributed over the 49-cell simulation area, which is 6 km<sup>2</sup>. Therefore, a network load of 1200 users represents a user density of 198 users/km<sup>2</sup>. The table shows that the DCA algorithms can cope with more users than the FCA algorithm under both uniform and nonuniform traffic distributions.

While this table is useful for finding the amount of traffic that can be handled under certain constraints, it can give misleading impressions. For example, the two LOLIAs with different exclusion zones ( $n = 7, 19$ ) seem to have a similar performance. However, this is a somewhat simplistic view, since the LOLIA with the larger exclusion zone ( $n = 19$ ) has a better quality of service than the other LOLIA ( $n = 7$ ), at the expense of higher probability of blocking new calls. The two LOLIAs appear to have a similar performance, since the capacity of the LOLIA using  $n = 19$  is limited by the new call blocking performance, whereas the LOLIA with  $n = 7$  is constrained by the low-quality access constraint. This implies that the network capacity of the LOLIA, with an exclusion zone of seven base

stations, is limited by the levels of interference. Hence, the addition of adaptive antennas increased the network capacity significantly, as can be clearly seen in Table III. In fact, an increase in the number of supported users of between 50–60% was observed for a four-element adaptive antenna array. The FCA algorithm with a seven-cell cluster size also benefitted significantly through the use of adaptive antenna arrays at the base stations, with an additional 100% of users served. However, the network capacity of the FCA algorithm using a 12-cell reuse pattern was not enhanced by the implementation of adaptive antennas, since its capacity was restricted by the new call blocking probability. These differences between the two FCA algorithms are confirmed by their performances in the shadowing environment, with the 12-cell cluster size variant performing better due to its greater reuse distance, leading to lower levels of interference. The LOLIA supports the higher number of users in the shadowing environment due to its dynamic configurability and goal of interference minimization. The network capacity of the LFA is limited to less than 500 users in the conservative scenario, but in the lenient scenario 1430 users are supported. This is due to the probability of low-quality access metric (not shown), which only dipped below 1% with less than 500 users.

Table III also demonstrates that the LOLIA can maintain the required performance constraints for the highest number of users in both the conservative and lenient scenarios, and with both uniform and nonuniform traffic distributions. In addition, the table shows that the DCA algorithms that attempt to reduce the interference, like LIA, LTA, and LOLIA, typically achieve a better overall performance than the radio spectrum packing algorithms, such as LOMIA and MTA.

In addition, the table shows the large increases in network capacity that can be obtained through the use of adaptive modulation. The network capacity of the FCA algorithm was limited by its network performance (as opposed to a data throughput restriction of 2 bits/s) and hence, at its maximum capacity, provided a mean data throughput of between 2.6 and 2.9 bits/s. However, the LOLIA exploited the network to a greater extent due to its dynamic nature, which resulted in a network performance limited by the mean data throughput for the two-antenna-element case. Hence, for the two-element adaptive antenna array, the change in mean modem throughput was 0%, but an additional 87% of network users were supported. The network using four-element adaptive antenna arrays exhibited a 59% gain in the number of supported users while benefitting from a 6.5% improvement in mean modem throughput.

### V. CONCLUSION

In this paper, we have discussed various DCA techniques and compared their performance to FCA both with and without shadow fading and under both uniform and nonuniform traffic distributions, using the performance metrics of Section III-A. The various channel allocation algorithms have different and sometimes opposite aims; hence a variety of performance metrics were required to quantify their performance.

The dynamic nature and the small “exclusion zone” of the LOLIA using  $n = 7$  resulted in its superior performance under



TABLE III

MAXIMUM NUMBER OF MOBILE USERS THAT CAN BE SUPPORTED USING THE ALGORITHMS INVESTIGATED WHILE MEETING THE DESIRED SYSTEM CONSTRAINTS FOR UNIFORM TRAFFIC (UT) AND NONUNIFORM TRAFFIC (NUT) DISTRIBUTIONS. THE USERS IN THE SYSTEM ARE DISTRIBUTED OVER THE 49-CELL SIMULATION AREA, WHICH IS 6 km<sup>2</sup>. THE SIMULATION PARAMETERS WERE DESCRIBED IN TABLE I

Algorithm	Conservative		Lenient	
	$P_{FT} = 1\%$ , $P_{low} = 1\%$ $GOS=4\%$ , $P_B = 3\%$		$P_{FT} = 1\%$ , $P_{low} = 2\%$ $GOS=6\%$ , $P_B = 5\%$	
	UT	NUT	UT	NUT
FCA (n=7)	815	680	1115	990
FCA (n=7) 4 el. BF	1665	—	2375	—
FCA (n=12)	1335	—	1545	—
FCA (n=12) 4 el. BF	1335	—	1525	—
MTA/HTA	1450	—	1545	—
LFA	<500	—	1430	—
LOMIA (n=19)	1500	1455	2040	1575
LTA	1815	—	1840	—
LIA	1820	—	1850	—
LOLIA (n=7)	1855	1445	2100	1675
LOLIA (n=7) 4 el. BF	2815	—	3385	—
LOLIA (n=19)	1920	—	2020	—
FCA (n=7) 3dB Shadowing	400	—	400	—
FCA (n=12) 3dB Shadowing	745	—	745	—
LOLIA (n=7) 3dB Shadowing	1555	—	1555	—
LOMIA (n=19) 3dB Shadowing	315	—	315	—
FCA (n=7) AQAM 2 el. BF	2390	—	2740	—
FCA (n=7) AQAM 4 el. BF	2490	—	2840	—
LOLIA (n=7) AQAM 2 el. BF	4340	—	4340	—
LOLIA (n=7) AQAM 4 el. BF	4585	—	4585	—

both uniform and nonuniform traffic conditions, and also in a slow fading propagation environment. The LOMIA with  $n = 19$  offered similar performance under nonuniform traffic conditions and under the uniform traffic distribution in the lenient scenario. However, the LOMIA did not perform well in the shadowing environment, with the LOLIA offering a significantly higher network capacity in the shadowing environment than the FCA algorithm or the LOMIA.

The benefits of using adaptive antenna arrays have been demonstrated, with improved network quality for an increased number of users, for both the FCA algorithm and the LOLIA. These benefits were then extended through the use of adaptive modulation to further improve call quality while simultaneously increasing the data throughput and the number of users adequately supported by the network.

A range of interesting further research problems arise when these algorithms are combined with statistical multiplexing algorithms or when burst-by-burst adaptive modems and slot classification algorithms are invoked, where more robust modem modes can be employed in strongly interfered channels while supporting more bandwidth-efficient modem modes in uninterfered slots. Exploiting the spatial dimension with the aid of adaptive antennas is also a promising research area.

#### ACKNOWLEDGMENT

The authors would like to thank the EPSRC, U.K., and the Virtual Centre of Excellence in Mobile Communications, U.K. They would also like to thank numerous professional friends for fruitful discussions.

#### REFERENCES

- [1] E. Sourour, "Time slot assignment techniques for TDMA digital cellular systems," *IEEE Trans. Veh. Technol.*, vol. 43, pp. 121–127, Feb. 1994.
- [2] S. W. Wales, "Technique for cochannel interference suppression in TDMA mobile radio systems," *Proc. Inst. Elect. Eng. Commun.*, vol. 142, no. 2, pp. 106–114, 1995.
- [3] J. Litva and T. Lo, *Digital Beamforming in Wireless Communications*. Norwood, MA: Artech House, 1996.
- [4] L. Godara, "Applications of antenna arrays to mobile communications, part I: Performance improvement, feasibility, and system considerations," *Proc. IEEE*, vol. 85, pp. 1029–1060, July 1997.
- [5] —, "Applications of antenna arrays to mobile communications, part II: Beam-forming and direction-of-arrival considerations," *Proc. IEEE*, vol. 85, pp. 1193–1245, Aug. 1997.
- [6] S. Tekinay and B. Jabbari, "A measurement-based prioritization scheme for handovers in mobile cellular networks," *IEEE J. Select. Areas Commun.*, vol. 10, no. 8, pp. 1343–1350, 1992.
- [7] G. P. Pollini, "Trends in handover design," *IEEE Commun. Mag.*, vol. 34, pp. 82–90, Mar. 1996.
- [8] R. C. Bernhardt, "Timeslot re-assignment in a frequency reuse TDMA portable radio system," *IEEE Trans. Veh. Technol.*, vol. 41, pp. 296–304, Aug. 1992.
- [9] J. C. I. Chuang, "Performance issues and algorithms for dynamic channel assignment," *IEEE J. Select. Areas Commun.*, vol. 11, pp. 955–963, Aug. 1993.
- [10] J. C. I. Chuang and N. R. Sollenberger, "Performance of autonomous dynamic channel assignment and power control for TDMA/FDMA wireless access," *IEEE J. Select. Areas Commun.*, vol. 12, pp. 1314–1323, Oct. 1994.
- [11] M. M. L. Cheng and J. C. I. Chuang, "Performance evaluation of distributed measurement-based dynamic channel assignment in local wireless communications," *IEEE J. Select. Areas Commun.*, vol. 14, pp. 698–710, May 1996.
- [12] L. Hanzo, P. Cherriman, and J. Streit, *Wireless Video Communications: From Second to Third Generation Systems and Beyond*. New York: IEEE Press, 2001.
- [13] L. Hanzo, W. T. Webb, and T. Keller, *Single- and Multi-Carrier Quadrature Amplitude Modulation*. New York: Wiley, 2000.

- [14] E. D. Re, R. Fantacci, and G. Giambene, "Handover and dynamic channel allocation techniques in mobile cellular networks," *IEEE Trans. Veh. Technol.*, vol. 44, pp. 229–237, May 1995.
- [15] I. ChihLin and C. PiHui, "Local packing—Distributed dynamic channel allocation at cellular basestation," in *Proc. IEEE Globecom '93*, vol. 1, Houston, TX, Nov. 29–Dec. 2 1993, pp. 293–301.
- [16] L. C. Godara, "Applications of antenna arrays to mobile communications, part I: Performance improvement, feasibility, and system considerations," *Proc. IEEE*, vol. 85, pp. 1029–1060, July 1997.
- [17] J. H. Winters, "Smart antennas for wireless systems," *IEEE Personal Commun.*, vol. 5, pp. 23–27, Feb. 1998.
- [18] D. Gerlach and A. Paulraj, "Adaptive transmitting antenna arrays with feedback," *IEEE Signal Processing Lett.*, vol. 1, pp. 150–152, Oct. 1994.
- [19] —, "Basestation transmitting antenna arrays for multipath environments," *Signal Process.*, pp. 59–73, 1996.
- [20] L. Hanzo and J. Stefanov, "The pan-European digital cellular mobile radio system—Known as GSM," in *Mobile Radio Communications*, R. Steele and L. Hanzo, Eds. Piscataway, NJ: IEEE Press, 1999, ch. 8, pp. 677–765.
- [21] W. C. Jakes, Ed., *Microwave Mobile Communications*. New York: Wiley, 1974.
- [22] S. Tekinay and B. Jabbari, "Handover and channel assignment in mobile cellular networks," *IEEE Commun. Mag.*, pp. 42–46, Nov. 1991.
- [23] I. Katzela and M. Naghshineh, "Channel assignment schemes for cellular mobile telecommunication systems: A comprehensive survey," *IEEE Personal Commun.*, pp. 10–31, June 1996.
- [24] J. Liberti and T. Rappaport, "A geometrically based model for line-of-sight multipath radio channels," in *Proc. VTC*, 1996, pp. 844–848.
- [25] R. Ertel, P. Cardieri, K. Sowerby, T. Rappaport, and J. Reed, "Overview of spatial channel models for antenna array communications systems," *IEEE Personal Commun.*, pp. 10–22, Feb. 1998.
- [26] R. Kohno, "Spatial and temporal communication theory using software antennas for wireless communications," in *Wireless Communications: TDMA Versus CDMA*. Norwood, MA: Kluwer, 1997, ch. 1, pp. 293–321.
- [27] Y. Ogawa and T. Ohgane, "Adaptive antennas for future mobile radio," *IEICE Trans. Fundamentals*, pp. 961–967, July 1996.
- [28] A. S. Tanenbaum, "Introduction to queueing theory," in *Computer Networks*, 2nd ed. Englewood Cliffs, NJ: Prentice-Hall, 1989, pp. 631–641.

**Jonathan Blogh** received the M.Eng. degree (with distinction) in information engineering and the Ph.D. degree in mobile communications, both from the University of Southampton, U.K., in 1997 and 2000, respectively.

His current areas of research include the networking aspects of FDD and TDD mode third-generation mobile cellular networks.

Mr. Blogh received the Lord Lloyd of Kilgerran Memorial Prize from the Institute of Electrical Engineering, U.K., in 1997 for interest and commitment to mobile radio and RF engineering.

**Peter Cherriman** received the M.Eng. degree in information engineering from the University of Southampton, U.K., in 1994, where he is currently pursuing the Ph.D. degree in mobile video networking in the Department of Electronics and Computer Science.

Currently, he is working on projects for the Mobile Virtual Centre of Excellence, U.K. His current areas of research include robust video coding, microcellular radio systems, power control, dynamic channel allocation, and multiple-access protocols.

**Lajos Hanzo** (M'91–SM'92) received the Masters degree (Dipl. Ing.) in electronics and the Ph.D. degree, both from the Technical University of Budapest, Hungary, in 1976 and 1983, respectively.

During his 24-year career in telecommunications, he has held various research and academic posts in Hungary, Germany, and the United Kingdom. Since 1986, he has been with the Department of Electronics and Computer Science, University of Southampton, U.K., and has been a Consultant to Multiple Access Communications Ltd., U.K. Currently, he holds the Chair in telecommunications. He has coauthored five books on mobile radio communications, published in excess of 300 research papers, organized and chaired conference sessions, presented overview lectures, and was awarded a number of distinctions. Currently, he is managing a research team working on a range of research projects in the field of wireless multimedia communications under the auspices of the Engineering and Physical Sciences Research Council, U.K., the European IST Programme, and the Mobile Virtual Centre of Excellence. He also provides a range of industrial training courses.